

Apremilast is a selective PDE4 inhibitor with regulatory effects on innate immunity



P.H. Schafer^{a,*}, A. Parton^a, L. Capone^a, D. Cedzik^a, H. Brady^a, J.F. Evans^b, H.-W. Man^c, G.W. Muller^d, D.I. Stirling^e, R. Chopra^a

^a Department of Translational Development, Celgene Corporation, Summit, NJ, USA

^b Department of Biology, PharmAkea, San Diego, CA, USA

^c Department of Process Chemistry, Celgene Corporation, Summit, NJ, USA

^d GWM Consulting, Rancho Santa Fe, CA, USA

^e BioTheryX, Inc., Chappaqua, NY, USA

ARTICLE INFO

Article history:

Received 11 February 2014

Received in revised form 22 May 2014

Accepted 23 May 2014

Available online 29 May 2014

Keywords:

Apremilast

Phosphodiesterase inhibitor

Preclinical drug evaluation

Psoriasis

Psoriatic arthritis

Spondyloarthropathies

ABSTRACT

Apremilast, an oral small molecule inhibitor of phosphodiesterase 4 (PDE4), is in development for chronic inflammatory disorders, and has shown efficacy in psoriasis, psoriatic arthropathies, and Behçet's syndrome. In March 2014, the US Food and Drug Administration approved apremilast for the treatment of adult patients with active psoriatic arthritis. The properties of apremilast were evaluated to determine its specificity, effects on intracellular signaling, gene and protein expression, and in vivo pharmacology using models of innate and adaptive immunity. Apremilast inhibited PDE4 isoforms from all four sub-families (A1A, B1, B2, C1, and D2), with IC₅₀ values in the range of 10 to 100 nM. Apremilast did not significantly inhibit other PDEs, kinases, enzymes, or receptors. While both apremilast and thalidomide share a phthalimide ring structure, apremilast lacks the glutarimide ring and thus fails to bind to cereblon, the target of thalidomide action. In monocytes and T cells, apremilast elevated intracellular cAMP and induced phosphorylation of the protein kinase A substrates CREB and activating transcription factor-1 while inhibiting NF-κB transcriptional activity, resulting in both up- and down-regulation of several genes induced via TLR4. Apremilast reduced interferon-α production by plasmacytoid dendritic cells and inhibited T-cell cytokine production, but had little effect on B-cell immunoglobulin secretion. In a transgenic T-cell and B-cell transfer murine model, apremilast (5 mg/kg/day p.o.) did not affect clonal expansion of either T or B cells and had little or no effect on their expression of activation markers. The effect of apremilast on innate immunity was tested in the ferret lung neutrophilia model, which allows monitoring of the known PDE4 inhibitor gastrointestinal side effects (nausea and vomiting). Apremilast significantly inhibited lung neutrophilia at 1 mg/kg, but did not induce significant emetic reflexes at doses <30 mg/kg. Overall, the pharmacological effects of apremilast are consistent with those of a targeted PDE4 inhibitor, with selective effects on innate immune responses and a wide therapeutic index compared to its gastrointestinal side effects.

© 2014 The Authors. Published by Elsevier Inc. This is an open access article under the CC BY license (<http://creativecommons.org/licenses/by/3.0/>).

Abbreviations: ANOVA, analysis of variance; ATF-1, activating transcription factor-1; CCL-2, chemokine ligand 2; CCL-8, chemokine ligand 8; CCL-18, chemokine ligand 18; CCR-1, chemokine receptor 1; CRBN, cereblon; CRE, cAMP responsive element; CREB, cAMP responsive element binding protein; CXCL-5, CXC cytokine ligand 5; DCs, dendritic cells; DMSO, dimethyl sulfoxide; EC₅₀, half-maximal effective concentration; ED₅₀, half-maximal effective drug concentration; ELISA, enzyme-linked immunosorbent assay; Epac, exchange proteins activated by cAMP; FP, fluorescence polarization; HEL, hen egg lysozyme; IC₅₀, half-maximal inhibitory concentration; Ig, immunoglobulin; IL, interleukin; IP-10, interferon-inducible protein 1; LPS, lipopolysaccharide; MCP-1, monocyte chemoattractant protein 1; MCP-2, monocyte chemoattractant protein 2; MHC, major histocompatibility complex; MIP-1αR, macrophage inflammatory protein 1-α receptor; MIP-4, macrophage inflammatory protein-4; MX1, myxovirus resistant 1; NF-κB, nuclear factor-kappa B; NK, natural killer; OVA, ovalbumin; PBMCs, peripheral blood mononuclear cells; PBS, phosphate-buffered saline; PDE4, phosphodiesterase 4; PKA, protein kinase A; PsA, psoriatic arthritis; SOCS-3, suppressor of cytokine signaling 3; TLR, toll-like receptor; TNF, tumor necrosis factor.

* Corresponding author at: Celgene Corporation, Department of Translational Development, 86 Morris Avenue, Summit, NJ 07901, USA. Tel.: +1 908 673 9166; fax: +1 908 673 2792.

E-mail address: pschafer@celgene.com (P.H. Schafer).

1. Introduction

Inflammatory conditions, such as psoriasis and psoriatic arthritis (PsA), are related to a dysregulated immune system governed by a pro-inflammatory cytokine network [1–3]. The network of pro-inflammatory mediators that drive psoriasis and PsA are released by a variety of cell types, including innate or adaptive immune cells, and resident non-immune cells [1–3]. The cyclic nucleotides cAMP and cGMP are naturally occurring intracellular secondary messengers critical to translating extracellular stimuli into intracellular signals that control gene expression, allowing the cell to interact with its environment and regulate broader physiological processes, including those involved in inflammation [4]. In the presence of inflammatory extracellular signals, G-protein-coupled receptors bind with a variety of ligands, such as leukotrienes, prostaglandins, chemokines, and histamine, and activate adenylyl cyclase, which promotes increased production of cAMP [5]. cAMP interacts with effector proteins such as protein kinase A (PKA) and exchange proteins activated by cAMP (Epac) to elicit changes in gene expression [6]. PKA activation results in phosphorylation of the cAMP-responsive binding element family of transcription factors, including cAMP responsive element binding protein (CREB) and activating transcription factor-1 (ATF-1), while inhibiting activity of other promoters such as nuclear factor kappa B (NF- κ B) [3,7,8]. Such effects on CREB, ATF-1, and NF- κ B cause decreased mRNA expression of cytokines and other inflammatory mediators as well as increased expression of anti-inflammatory signals [5,8]. In this way, cAMP signaling helps to maintain immune homeostasis by modulating the production of pro-inflammatory and anti-inflammatory mediators [5]. When intracellular cAMP concentrations are high, inflammatory signaling is dampened; likewise, when cAMP levels are depleted, expression of inflammatory mediators increases. By modulating the levels of inflammatory and anti-inflammatory mediators expressed and released by immune cells, cAMP is one component in a cascade that determines recruitment of immune responses both in the local milieu and throughout the body.

Intracellular levels of cAMP are tightly controlled by adenylyl cyclase, which promotes cAMP formation, and by cyclic nucleotide phosphodiesterases (PDEs), which are the only means of degrading cAMP, via enzymatic hydrolysis. There are 11 distinct families of cAMP and/or cGMP-selective PDEs expressed in mammalian species (PDE1–11), each containing a conserved catalytic domain in the carboxy-terminal portion of the enzyme, plus amino-terminal subdomains that are important for subcellular localization, and for interactions with signaling molecules and molecular scaffolds [9]. While certain PDEs specifically hydrolyze cAMP (PDE4, PDE7, and PDE8), or specifically hydrolyze cGMP (PDE5, PDE6, and PDE9), others hydrolyze both cAMP and cGMP (PDE1, PDE2, PDE3, PDE10, and PDE11) [9]. In most mammalian cells, PDE3 and PDE4 predominantly hydrolyze cAMP [9]. Unlike PDE3, PDE4 is cAMP-specific and the dominant PDE in inflammatory cells [3, 10]. PDE4 is also expressed in structural cell types involved in psoriasis, such as keratinocytes, vascular endothelium, and synovium [11]. The PDE4 isoenzyme family is encoded by four genes (PDE4A, PDE4B, PDE4C, and PDE4D) and consists of more than 20 distinct isoforms, each with a unique N-terminal region, created by mRNA splicing and different promoters [4,12]. PDE4 isoforms are categorized as long, short, or super short depending on the presence and number of upstream conserved regions, highly conserved domains located between the catalytic domain and the N-terminal region; dead-short isoforms are those containing no upstream conserved regions and a truncated, nonfunctional catalytic domain [13]. In line with the structural diversity of the PDE4 family, the unique N-terminal region of each PDE4 isoform allows each to be sequestered by specific protein partners within sub-regions of the cell [12]. PDE4 inhibition elevates intracellular cAMP levels, which results in down-regulation of the inflammatory responses by reducing the expression of tumor necrosis factor (TNF)- α , interleukin (IL)-23, and other pro-inflammatory cytokines, while

increasing anti-inflammatory cytokines, such as IL-10 [3,14]. Therefore, PDE4 is of interest as a therapeutic target in the treatment of chronic inflammatory conditions [14,15]. Currently marketed PDE4 inhibitors include apremilast (Otezla®, Celgene Corporation, Summit, New Jersey) [16], approved in the United States for the treatment of adult patients with active PsA, and roflumilast (Daliresp®, Forest Pharmaceuticals, St. Louis, Missouri) [17] for the treatment of chronic obstructive pulmonary disorder.

Apremilast is an oral small molecule inhibitor of PDE4 [11,15,18] which has been shown to be effective and well tolerated in clinical trials in psoriasis (phase III), PsA (phase III), and Behçet's disease (phase II). Targeted inhibition of PDE4 results in partial inhibition of pro-inflammatory mediator production, such as TNF- α , interferon- γ , and IL-23, and increases in anti-inflammatory mediator production, such as IL-10 [3,15,19], which in turn results in reduced infiltration of immune cells and changes in resident cells of the skin and joints [11,15, 19,20]. In vitro, apremilast significantly reduced expression of TNF- α , IL-7, and the matrix metalloproteinases MMP1, MMP3, MMP13, and MMP14 by synoviocytes derived from patients with rheumatoid arthritis [19,21,22]. In other cell culture models, apremilast inhibited the differentiation of osteoclasts, as well as their bone-resorbing activity, and reduced the production of RANKL by osteoblasts [23]. In patients with severe plaque psoriasis, apremilast reduced infiltration of myeloid dendritic cells (DCs) into the dermis and epidermis and inducible nitric oxide synthase mRNA expression; epidermal thickness was reduced by approximately 20% over 29 days [20]. A subsequent study in recalcitrant plaque psoriasis demonstrated that apremilast reduced epidermal and dermal infiltration of myeloid DCs, T cells, and natural killer (NK) cells, and inhibited the expression of genes in the Th1, Th17, and Th22 pathways in the psoriatic skin lesions, including IL-12/IL-23p40, IL-23p19, IL-17A, and IL-22 [24]. Phase II and phase III studies have demonstrated the clinical efficacy of apremilast in the treatment of patients with active PsA and moderate to severe plaque psoriasis, and phase II studies have demonstrated the efficacy of apremilast for patients with Behçet's disease [25–33].

The current analyses studied the pharmacodynamic properties of apremilast, with three specific aims: 1) ascertain the selectivity of apremilast by determining whether it binds to targets other than PDE4 in the cell; 2) define which signaling pathways downstream of PDE4 are modulated by apremilast; and 3) identify the repertoire of immune cells affected by the drug. Our data show that apremilast has no identified binding targets other than PDE4 and mediates its effects in monocytes and T cells via PKA and NF- κ B pathways. Apremilast modulates gene expression in monocytes, reduces interferon- α production induced by TLR9 signaling in plasmacytoid DCs, and inhibits cytokine production by T cells, but has little effect on immunoglobulin secretion by B cells in vitro. To assess its impact on the adaptive immune response, apremilast was tested in an antigen-specific transgenic mouse model of T- and B-cell clonal expansion, activation marker expression, and immunoglobulin production. Using the ferret as both a model of an innate inflammatory response, and for the gastrointestinal side effects of PDE4 inhibition, a therapeutic index was measured in vivo.

2. Material and methods

2.1. Materials

Celgene Corporation (Summit, New Jersey) synthesized apremilast (CC-10004 or [S]-N-[2-[1-3-ethoxy-4-methoxyphenyl]-2-methanesulfonylethyl]-1,3-dioxo-2,3-dihydro-1H-indol-4-yl] acetamide) and other PDE4 inhibitors, as well as thalidomide, lenalidomide (CC-5013), and pomalidomide (CC-4047). Forskolin was obtained from Sigma (St. Louis, Missouri) and dimethyl sulfoxide (DMSO), used to generate stock solutions, was obtained from Research Organics (Cleveland, Ohio).

2.2. Methods

2.2.1. PDE selectivity

Apremilast (10 μ M) PDE enzyme specificity was assessed against recombinant human PDEs 1A, 1C, 2A, 3A, 3B, 4A1A, 4B1, 4B2, 4C1, 4D2, 5A1, 7A, 7B, 8A1, 9A2, 10A1, and 11A4 using IMAP™ TR-FRET Screening Express with Progressive Binding Kit (Molecular Devices, Sunnyvale, California). The PDE4 isoforms examined included long isoforms PDE44B1 [34] and PDE44C1 [35], the short isoforms PDE4B2 [36] and PDE4D2 [37], and the super-short isoform PDE4A1A [38]. The enzymatic reactions were conducted at room temperature for 1 h in a 50 μ L mixture of IMAP reaction buffer, 100 nM FAM-cAMP, or 100 nM FAM-cGMP, test compound, and a PDE enzyme. Fluorescence intensity was measured at an excitation of 485 nm and an emission of 528 nm using a BioTek Synergy™ 2 microplate reader and converted to fluorescence polarization (FP) using Gen5 software. The highest value of FP in each data set was defined as 100% activity, and the percent binding activity in the presence of compound was calculated by $(FP \text{ in presence of compound} - FP \text{ in absence of PDE enzyme and compound}) / (\text{highest FP} - FP \text{ in presence of compound}) \times 100\%$. PDE6 enzymatic activity was measured enzymatically using PDE6 isolated from bovine retinal rod outer segments at 100 μ M cGMP for 20 min at 25 °C (MDS Pharma, Bothell, Washington).

The kinase inhibition profile of 10 μ M apremilast was determined using the SelectScreen® Profiling Service (Invitrogen, Carlsbad, California), which included 255 kinases. Significant kinase inhibition was considered to be reproducible inhibition of 50% or more at 10 μ M.

The effects of 10 μ M apremilast on binding to 68 cell surface receptors and for inhibition of 17 enzymes were tested (Cerep Diversity Profile, Cerep SA, Poitiers, France, and Cerep, Inc., Seattle, Washington). Receptors tested include adenosine, adrenergic, angiotensin, benzodiazepine, bradykinin, cannabinoid, cholecystokinin, corticotrophin-releasing factor, dopamine, endothelin, γ -aminobutyric acid, α -amino-3-hydroxy-5-methyl-4-isoxazolepropionic acid, kainite, N-methyl-D-aspartate, histamine, imidazoline, leukotriene, melanocortin, muscarinic, neurokinin, neuropeptide Y, opioid, nociceptin, phencyclidine, purinergic, serotonin, glucocorticoid, estrogen, progesterone, androgen, thyrotropin-releasing hormone, and vasopressin, and ion channels, including calcium, sodium, chloride, and potassium, transporters including norepinephrine, dopamine, γ -aminobutyric acid, choline, and serotonin. Enzymes included phosphodiesterases, adenylyl cyclase, guanylyl cyclase, protein kinase C, acetylcholinesterase, catechol-O-methyl transferase, γ -aminobutyric acid transaminase, monoamine oxidases, phenylethanolamine-N-methyl transferase, tyrosine hydroxylase, and ATPase. Receptor binding by a specific ligand was defined as the difference between the total binding and the nonspecific binding determined in the presence of an excess of unlabeled ligand. Results were expressed as a percent inhibition of control specific binding or as a percent variation of control values obtained in the presence of apremilast.

Competition studies with cereblon binding to thalidomide-analog affinity beads were performed using varying concentrations of apremilast, lenalidomide (positive control), and DMSO (control) preincubated (15 min at room temperature) with human U266 multiple myeloma cell extract (American Type Cell Culture, Manassas, Virginia) containing cereblon. Thalidomide analog-coupled beads were prepared using ferrite glycidyl methacrylate affinity beads, as described by Ito et al. [39]. Beads were added to protein extracts, and the samples were rotated for 2 h at 4 °C and then washed three times. The bound proteins were eluted with sodium dodecyl sulfate polyacrylamide gel electrophoresis sample buffer and cereblon binding was quantified by two independent immunoblots using the anti-cereblon monoclonal antibody CRBN 65–76 (1:10,000). Cereblon signal density relative to control density was graphed using PrismGraph nonlinear regression analysis set at log inhibitor versus response with a variable slope and bottom constraint set to zero. The PrismGraph program calculated standard error of the mean for each compound concentration point.

2.2.2. cAMP elevation

Human peripheral blood mononuclear cells (PBMCs) were isolated by Ficoll gradient from source leukocytes (buffy coat) and plated in 96-well plates at 1×10^6 cells per well in RPMI-1640. The cells were pre-treated with compounds at 100, 10, 1, 0.1, 0.01, 0.001, 0.0001, and 0 μ M in a final concentration of 2% DMSO in duplicate at 37 °C in a humidified incubator at 5% CO₂ for 1 h. The cells were then stimulated with prostaglandin E2 (10 μ M) (Sigma) for 1 h. The cells were lysed with HCl, 0.1 N final concentration to inhibit PDE activity, and the plates were frozen at –20 °C. The cAMP produced was measured using cAMP (low pH) immunoassay kit (R&D Systems, Minneapolis, Minnesota). cAMP levels were normalized to the level induced by prostaglandin E2 in the presence of 100 μ M rolipram.

2.2.3. LPS-induced TNF- α production

PBMC production of TNF- α induced by lipopolysaccharide (LPS) was performed as previously described [15].

2.2.4. Plasmacytoid DC interferon- α production

The effect of apremilast on interferon- α production by plasmacytoid DCs was assessed in PBMCs stimulated via TLR9. PBMCs were isolated from donor-collected peripheral blood. Cells were pretreated with apremilast for 1 h before stimulation with the TLR9 agonist CpG-A oligodeoxynucleotide 2216 (InvivoGen, San Diego, California) over 16 h. Using an enzyme-linked immunosorbent assay (ELISA), the optimal concentration of CpG-A oligodeoxynucleotide 2216 was identified as 1 μ M for interferon- α production from PBMCs (109 pg/mL). At the end of the treatment period, supernatant was collected for analysis of interferon- α production using ELISA (Pierce Chemical Company, Rockford, Maryland). The half-maximal inhibitory concentration (IC₅₀) was calculated from the non-linear regression, sigmoidal dose response curves constraining the minimum of 0% and maximum of 100% (GraphPad Prism v4.0, San Diego, California).

2.2.5. B-cell immunoglobulin production

The effects of apremilast on B-cell differentiation were studied in PBMCs and compared with pomalidomide. B cells were isolated from PBMCs and activated with a cocktail of IL-2, IL-10, IL-15, CD40 ligand/TNFSF5/histidine-tagged polyHistidine mouse IgG1 antibody, and oligodeoxynucleotide 2006-human TLR9 ligand. Apremilast, pomalidomide, or DMSO was added to each well of a six-well flat-bottom plate and incubated for 4 days at 37 °C. Cells were harvested and washed with phosphate-buffered saline (PBS), and a fresh B-cell cocktail of IL-2, IL-10, IL-15, and IL-6 was added to the cells. Test compounds were again added and incubated for 3 days at 37 °C. On Day 7, supernatants were harvested and analyzed by ELISA for IgG and IgM production (ZeptoMetrix Corporation, Buffalo, New York). IC₅₀ was calculated from the non-linear regression, sigmoidal dose response curves constraining the minimum of 0% and maximum of 100% (GraphPad Prism v5.0). Results were expressed as the percent inhibition relative to control DMSO values or as present expression calculated relative to the DMSO control (100% expression).

2.2.6. T-cell cytokine production

T cells were isolated from buffy coat by negative selection using the RosetteSep T Cell Enrichment Cocktail (STEMCELL Technologies, Vancouver, British Columbia, Canada) according to manufacturer's procedures. All 96-well plates were pre-coated with 3 μ g/mL anti-human CD3 antibody OKT3 clone (eBioscience, Cat# 16-0037-85) in 100 μ L 1 \times PBS for 4 h at 37 °C. The plates were washed three times with RPMI-1640 Complete Media before the T-cell assay. The T cells were then plated in anti-CD3-pre-coated plates at a density of 2.5×10^5 cells/well in 180 μ L RPMI-1640 Complete Media. The cells were treated with 20 μ L 10 \times compounds. The final DMSO concentration was 0.25%. The plates were incubated for 48 h at 37 °C, 5% CO₂. After 48 h, the supernatants were harvested and tested by a multiplex

cytometric bead array assay using the Luminex Human Cytokine/Chemokine 12-Plex Kit (Cat# MPXHCYTO-60K-12, Millipore, Billerica, Massachusetts) and analyzed on a Luminex IS100 instrument (Millipore).

2.2.7. Gene expression in monocytes

The effects of apremilast (1 μ M) on gene expression were studied in a gene chip analysis and compared with the thalidomide analogs lenalidomide (10 μ M) and pomalidomide (1 μ M), the PDE4 inhibitors roflumilast (0.1 nM) and cilomilast (1 μ M), and the c-Jun N-terminal inhibitor CC-225400 (10 μ M). CD14+ monocytes were isolated from PBMCs from four donors, and the RNA was pooled. Cells were pretreated with compounds for 1 h and then stimulated with 50 ng/mL LPS for 6 h. GeneChip Human Genome U133A array (Affymetrix, Santa Clara, California) encoding probes, representing approximately 13,000 unique human genes, were used. Gene expression data were analyzed and gene ontology pathways were compared using NextBio software (Illumina, Inc., San Diego, California). Based on results, a set of the most highly apremilast-modulated genes were chosen for confirmatory studies using real-time polymerase chain reaction analysis of mRNA expressed in LPS-stimulated human monocytes and human PBMCs. Statistical analysis was performed using two-way analysis of variance (ANOVA) Bonferroni post-test versus control.

2.2.8. Intracellular signaling

The intracellular mechanism of action of apremilast on the PKA and NF- κ B pathways was studied in Jurkat T-cell leukemia and THP-1 monocytic leukemia cell lines (American Type Cell Culture). Cells were cultured at 10 million cells per dish in 10 \times 10 cm tissue culture dishes in 10 mL Roswell Park Culture Medium-1640 Media (Mediatech Inc., Manassas, Virginia) and supplemented with 10% fetal bovine serum, 2 mM L-glutamine, 100 U/mL penicillin, and 100 μ g/mL streptomycin. The next day, the cells were treated with 0.1% DMSO (control), 0.1, 1, and 10 μ M apremilast, with and without the adenylyl cyclase activator forskolin (10 μ M), or 1, 0.1, and 0.01 μ M roflumilast. After 30 min, the cells were washed twice in ice-cold PBS, then lysed for 10 min in 200 μ L/sample pre-chilled 1 \times RIPA Buffer (Thermo Fisher, Waltham, Massachusetts) supplemented with 1 \times protease and phosphatase inhibitors. The lysates were vortexed for 30 s and centrifuged in a microcentrifuge at maximum speed (16,100 \times g) for 10 min at 4 $^{\circ}$ C. The BCA Assay Kit (Thermo Fisher) was used according to manufacturer's procedures to measure protein concentration.

To determine NF- κ B nuclear localization, Jurkat T cells and THP-1 monocytic cells were incubated under the same conditions with 10 μ M I κ B kinase inhibitor VII (Calbiochem, Billerica, Massachusetts). After a 1-hour incubation at 37 $^{\circ}$ C, Jurkat T cells were stimulated with 20 ng/mL recombinant human TNF- α (R&D Systems), and THP-1 cells were stimulated with 1 μ g/mL LPS *Escherichia coli* 0127:B8 (Sigma) for an additional hour. The cells were centrifuged at 1200 RPM (290 \times g) for 10 min and washed twice with cold 1 \times PBS (Mediatech Inc.). Cytoplasmic and nuclear proteins were isolated using the NE-PER Cytoplasmic and Nuclear Protein Extraction Kit (Thermo Fisher), following the manufacturer's procedure for 20 μ L packed cell volume, and the protein concentration was measured using the BCA Assay Kit, as described above.

Western blot was used to measure the phosphorylation of the PKA substrate CREB at Ser133 and NF- κ B p65. The lysates were run on 10% Tris-HCl pre-cast gels (Bio-Rad, Hercules, California) at 50 μ g protein per lane at 160 V until the protein of interest reached two thirds of the gel. The proteins were transferred to nitrocellulose membrane (Invitrogen, Grand Island, New York) and run at 100 V for 3 h on ice. After 3 h, the membranes were blocked using Odyssey Blocking Buffer (LI-COR, Lincoln, Nebraska) for 1 h at room temperature on a shaker and then they were probed with either phospho-CREB Ser122 Rabbit Antibody or NF- κ B p65 Rabbit Antibody (Cell Signaling, Danvers, Massachusetts) and incubated overnight at 4 $^{\circ}$ C with gentle shaking. The next

day, the membranes were washed and LI-COR secondary antibody goat anti-rabbit IRDye 680 LT (1:20,000) was added. After incubation and washing, the blots were analyzed on the LI-COR Odyssey instrument. The blots were stripped and re-probed with β -actin (1:20,000, Clone AC-15 produced in mouse; Sigma), incubated for 1 h on a shaker, and then washed. Secondary antibody goat anti-mouse IRDye 800 CW (LI-COR) was added and incubated for 30 min with gentle shaking. After washing, the blots were analyzed on the LI-COR Odyssey Imaging System. Densitometry was performed, and each band was normalized to the corresponding β -actin band.

Jurkat T cells and THP-1 cells were plated at a density of 100,000 cells per well in 100 μ L RPMI-1640 Media and incubated overnight at 37 $^{\circ}$ C, 5% CO₂. The wells were transfected with Superfect:DNA complex and incubated for 10 min at room temperature. After 10 min, the master mix of Opti-MEM Medium, Superfect reagent, and plasmid DNA stock was added to the plate, which was subsequently mixed, covered, and incubated for 24 h at 37 $^{\circ}$ C. The next day, 10 \times compound solutions and 10 \times inducing controls were prepared. The cells were pretreated with 10 μ L of 10 \times titrated compounds and 0.1, 1, and 10 μ M apremilast. After 1 h, Jurkat T cells were stimulated with 10 μ L of 10 \times recombinant human TNF- α , and THP-1 cells were stimulated with 10 μ L of 10 \times LPS and then incubated for 6 h at 37 $^{\circ}$ C. Luciferase activity was analyzed using the One-GloTM Luciferase Assay System (Promega, Madison, Wisconsin) according to the manufacturer's procedures. Each 100 μ L sample was placed in an Eppendorf tube and analyzed in duplicate on the single tube luminometer (Turner Designs TD-20/20) in standard mode.

2.2.9. Transgenic T- and B-cell model

Antigen-specific adaptive immune responses were studied using the transgenic mouse T- and B-cell transfer model with male and female IgHb mice (University of Glasgow, as previously described [40]). This study was conducted before the enactment of the EU Directive 2010/63/EU for animal experiments. The CD4+ T cells of the DO11.10 T-cell receptor-transgenic mice are specific for a chicken ovalbumin (OVA) peptide (amino acid residues 323–339) in the context of the MHCII molecule I-A^d and can be identified using the clonotypic monoclonal antibody KJ1–26 (referred to as KJ+ T cells). MD4 B-cell receptor-transgenic mice, which are specific for hen egg lysozyme (HEL), can be identified using an antibody specific for the IgM^a allotype (referred to as MD4+ B cells). During acclimation and after dosing, animals were housed in groups of 10 mice maximum in polypropylene cages (37.5 \times 21 \times 18 cm) fitted with solid bottoms and filled with wood shavings as bedding material. Mice were housed at 20 $^{\circ}$ C to 24 $^{\circ}$ C at 30% to 70% relative humidity and a 12:12 h light:dark cycle, and were provided a commercial high-fat rodent diet ad libitum and free access to drinking water, supplied to each cage via polyethylene bottles with stainless steel sipper tubes. Groups of 30 mice were randomly assigned to each of the four treatment regimens. On Day – 1, antigen-specific transgenic T and B cells were injected intravenously via the tail vein using 3 \times 10⁶ KJ+ T cells and 3.5 \times 10⁶ MD4+ B cells. On Day 0, mice were immunized by subcutaneous injection of 130 μ g OVA-HEL/Complete Freund's Adjuvant emulsion (per mouse). Mice were treated with apremilast (5 mg/kg) or the vehicle (0.5% carboxymethylcellulose/0.25% Tween 80) once daily commencing on Day – 1. At the end of the study, surviving animals were euthanized by cervical dislocation. On Day 2, sampling of inguinal, axillary, brachial lymph nodes was conducted using five mice per time point for flow cytometry to count KJ+ T cells and MD4+ B cells; for CD69, CD25 (IL-2 receptor), and CD62L (L-selectin) expression on the KJ+ T cells; and for CD40, CD80, CD86, and MHCII expression on IgM^a+ B cells.

2.2.10. Ferret lung neutrophilia and emesis model

Male ferrets (*Mustela putorius furo*, weighing 1 to 2 kg) were supplied either by Bury Green Farm (Hertfordshire, UK) or Misay Consultancy (Hampshire, UK). This study was conducted before the

enactment of the EU Directive 2010/63/EU for animal experiments. Following transport, the animals were allowed to acclimatize in the holding rooms for ≥ 7 days. Meals comprised SDS diet C pelleted food given ad lib with Whiskas cat food given three times per week. Pasteurized animal grade drinking water was changed daily. PDE4 inhibitors were administered orally (p.o.) at doses of 0.1 to 30 mg/kg (apremilast) or 1 to 10 mg/kg (cilomilast). Ferrets were fasted overnight but allowed free access to water. The animals were orally dosed with vehicle or PDE4 inhibitor using a 15 cm dosing needle that was passed down the back of the throat into the esophagus. After dosing, the animals were returned to holding cages fitted with acrylic doors to allow observation and given free access to water. After dosing, the animals were constantly observed and any emesis or behavioral changes were recorded. The total number of emetic episodes (retching and vomiting) was recorded. Thirty minutes after p.o. dosing with compound or vehicle control, the ferrets were exposed to an aerosol of LPS (100 $\mu\text{g}/\text{mL}$) for 10 min. Aerosols of LPS were generated by a nebulizer (DeVilbiss Healthcare, Somerset, Pennsylvania), which was directed into the acrylic exposure chamber. After a 10-minute exposure period, the animals were returned to the holding cages and allowed free access to water. The animals were allowed access to food 60 to 90 min after p.o. dosing. Observation continued for at least 2.5 h post-p.o. dosing, and emetic episodes and behavioral changes were recorded. Six hours after LPS exposure, the animals were killed by overdose of sodium pentobarbitone administered intraperitoneally. Tracheae were then cannulated with polypropylene tubing and lungs lavaged twice with 20 mL heparinized (10 U/mL) PBS. The bronchoalveolar lavage samples were centrifuged at 1500 rpm for 5 min. The supernatant was removed and the resulting cell pellet was re-suspended in 1 mL PBS. A cell smear of the re-suspended fluid was prepared and stained with Leishman's stain to allow differential cell counting. A total cell count was made using the remaining re-suspended sample. From this, the total number of neutrophils in the bronchoalveolar lavage was determined. The therapeutic index was calculated as the highest dose found to not cause emetic episodes divided by the lowest dose found to inhibit pulmonary neutrophilia by $\geq 50\%$.

3. Results

3.1. PDE selectivity

To determine the selectivity of apremilast among the various PDE families, both cAMP- and cGMP-hydrolyzing activity of PDEs 1–11 was tested. Several PDE4 isoforms were selected to represent the long (4B1, 4C1), short (4B2, 4D2), and super-short (4A1A) isoforms [13]. PDE4B1, PDE4B2, PDE4D1, and PDE4D2 are reported to be expressed in primary monocytes, macrophages, T cells, and neutrophils [41]. The super-short PDE4A1 isoform is unique in that it contains an N-terminal region that mediates its insertion into membranes and is found enriched in Golgi and associated vesicles [42]. The PDE assays confirmed apremilast to be a selective inhibitor of PDE4, with significant inhibition observed only for the PDE4 isozymes. Apremilast (10 μM) displayed an average of approximately 95% (range: 91%–99%) inhibition of the PDE4 enzymes (A1A, B1, B2, C1, and D2) (Fig. 1). Apremilast did not significantly inhibit the other PDEs tested. Concentration-dependent inhibition of these PDE4 isoforms was subsequently confirmed with apremilast IC_{50} values for PDE4A1A, PDE4B1, PDE4B2, PDE4C1, and PDE4D2 of 14, 43, 27, 118, and 33 nM. This inhibition pattern is consistent with the profile of a pan-PDE4 inhibitor, with some selectivity for the super-short PDE4A1A isoform.

Apremilast (10 μM) also did not significantly inhibit any of the 255 kinases tested. Apremilast (10 μM) had no significant activity against any of the cell surface receptors or enzymes tested in a broad-based screen, except for 95% inhibition of PDE4 (data not shown).

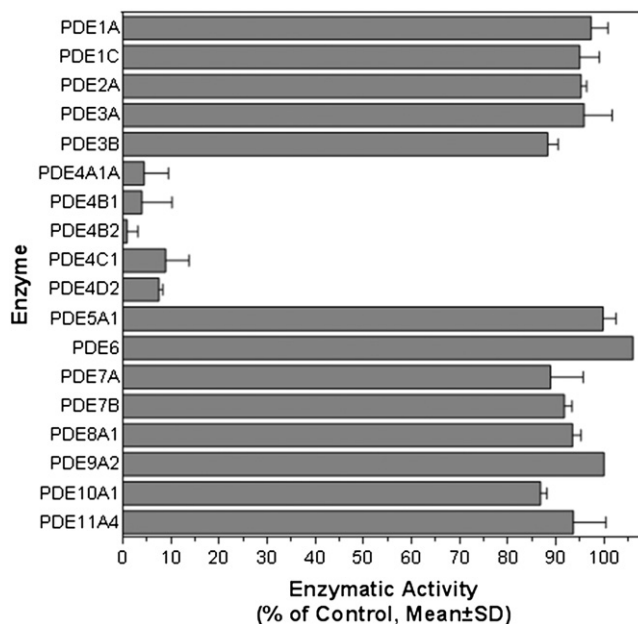


Fig. 1. Effect of apremilast on PDE enzyme activity. Apremilast (10 μM) was added to phosphodiesterases, and enzymatic activity was measured, as described in the [Material and methods](#) section. Enzymatic reactions were carried out in 100 nM cAMP as a substrate, except for PDE5A1 and PDE9A2 (100 nM cGMP) and retinal rod PDE6 (100 μM). Data are shown as the mean with the standard deviation from assays performed in duplicate.

Apremilast has previously been referred to as a thalidomide analog [43] because of their common structural feature, the phthalimide ring. Recently, the molecular target of thalidomide has been identified as cereblon, a component of an E3 ubiquitin ligase complex [39]. The binding of thalidomide to cereblon has been shown to be mediated through

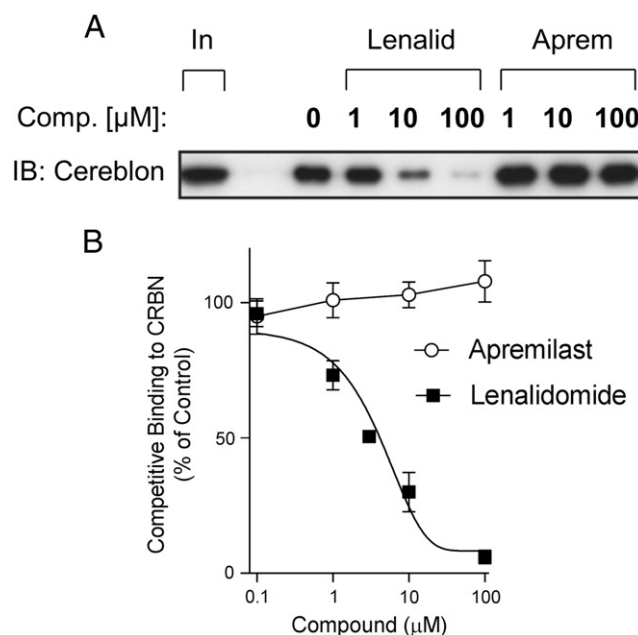


Fig. 2. Lack of apremilast binding to cereblon, the molecular target of thalidomide. **A**—Lenalidomide or apremilast was preincubated with human myeloma U266 cell extract containing cereblon and then incubated with thalidomide analog affinity beads. Beads were washed and then bound proteins were eluted, subjected to SDS-PAGE, and immunoblotted using an antibody against cereblon. In, input protein showing cereblon presence in the cell lysate. **B**—Experiments were performed as in **A** using lenalidomide and apremilast, and CRBN immunoblot band intensities were quantified. Data from two independent experiments with samples from each experiment subject to two independent immunoblots were used to calculate signal density relative to control density.

its glutarimide ring, rather than its phthalimide ring [39,44]. Because apremilast does not contain a glutarimide ring, it would not be expected to bind to cereblon. To confirm this hypothesis, apremilast was tested for cereblon binding affinity. In cereblon competition binding experiments, apremilast, at concentrations up to 100 μM , did not compete for the binding of U266 multiple myeloma cell-derived cereblon with the thalidomide analog affinity beads. In contrast, preincubation with lenalidomide did compete for cereblon binding, with approximately 50% inhibition at 3 μM (Fig. 2). These results demonstrate that apremilast does not bind to human cereblon.

3.2. cAMP elevation

Apremilast elevated intracellular cAMP in PBMCs in response to prostaglandin E2 in a manner similar to rolipram and cilomilast, with a half-maximal effective concentration (EC_{50}) of 1.4, 12, and 5 μM , respectively (Fig. 3). However, roflumilast elevated cAMP more potently with an EC_{50} of 68 nM, and to a level approximately 50% higher than that of rolipram. By contrast, thalidomide and its analogs, lenalidomide and pomalidomide, did not increase intracellular cAMP levels at any concentration up to 100 μM (Fig. 3), consistent with previous evidence showing these compounds lack PDE4 inhibitory activity [45].

3.3. Cellular effects by innate and adaptive immune cells in vitro

To study the effects of apremilast on innate and adaptive immune responses in vitro, and to compare it with the effects of the thalidomide analogs lenalidomide and pomalidomide, four cell culture models were used: 1) LPS-stimulated PBMCs, to induce TNF- α production via the TLR4 pathway in monocytes; 2) CpG oligonucleotide-stimulated PBMCs, to induce interferon- α production via the TLR9 pathway in plasmacytoid DCs; 3) B-cell stimulation with cytokines, CD40 ligand, and CpG, to induce differentiation and immunoglobulin secretion; and 4) CD3-antibody stimulated T cells, to induce IL-2 and other cytokine production. As previously reported, apremilast inhibited LPS-induced TNF- α production, as did the thalidomide analogs lenalidomide and pomalidomide, with an IC_{50} of 29 nM, 14 nM, and 2.7 nM, respectively (Fig. 4A). However, in CpG oligonucleotide-stimulated PBMCs, apremilast reduced interferon- α production with an IC_{50} of 0.62 μM , but lenalidomide had very modest effects, with only 28% reduction in interferon- α production at 10 μM (Fig. 4B). When added to the B-cell differentiation culture, apremilast had a modest effect on IgG production, with a maximal inhibition of 33% at 10 μM . By contrast, pomalidomide potently inhibited IgG production with an IC_{50} of 63 nM (Fig. 4C). In the T-cell cultures, apremilast inhibited IL-2 production with an IC_{50} of 2.4 μM , but

pomalidomide had the opposite effect, enhancing IL-2 production by almost 20-fold (Fig. 4D). A selection of Th1, Th2, and Th17 cytokines were also profiled in the T-cell cultures. Apremilast inhibited all T-cell-derived cytokines with a range of potencies, including the Th2 cytokines IL-5, IL-10, and IL-13 with an IC_{50} in the 30 to 280 nM range, the Th17 cytokine IL-17 with an IC_{50} of 90 nM, and the Th1 cytokines TNF- α , GM-CSF, and interferon- γ with an IC_{50} in the 0.93 to 1.3 μM range (Fig. 5). The least potent effect of apremilast was on the chemokine RANTES, with an IC_{50} of 4.1 μM . Thus, while both apremilast and the thalidomide analogs lenalidomide and pomalidomide can inhibit TLR4-dependent TNF- α production, these two classes of compounds are quite distinct in their effects on plasmacytoid DCs, B cells, and T cells.

To further explore the effects of apremilast and the thalidomide analogs lenalidomide and pomalidomide on TLR4-dependent signaling, gene expression profiling was conducted in purified monocytes stimulated with LPS and analyzed on the GeneChip Human Genome U133A array. Among the more than 39,000 transcripts represented on the gene array, only 20 were regulated in common by all six compounds: TNF, CCL8, P2RX7, FFAR2, VCAN, IL-12B, DENND2D, CXCL5, NBN, CCL15, IL-23A, HDAC9, SPP1, TFPI, JAKMIP2, CDC42EP3, NCF1, DUSP6, SGK, and RDH11 (Supplementary Table 1). Differences were clear between apremilast and the thalidomide analogs, with lenalidomide and pomalidomide demonstrating a gene modulation pattern more similar to each other than to apremilast (Fig. 6). The apremilast pattern was more similar to that of roflumilast and cilomilast, while the c-Jun N-terminal inhibitor produced a gene expression pattern unique to itself. In this study, apremilast modulated the expression of 498 genes by ≥ 1.7 -fold, and among the three PDE4 inhibitors, 239 genes were regulated in common (Supplementary Table 2). An analysis of the gene transcription, based on Gene Ontology and Broad MSigDB Canonical Pathways, identified the top gene sets regulated concordantly by all three PDE4 inhibitors as belonging to the immune response, inflammatory response, cytokine activity, chemokine signaling, and stress response biogroups (Table 1; Supplementary Table 3). In contrast, there were numerous gene sets regulated by cilomilast and roflumilast, but not by apremilast. The top gene sets reflecting this discordance among the PDE4 inhibitors belonged to the cytoplasmic ribosome, peptide chain elongation, ribosome, protein complex disassembly, and viral infectious cycle biogroups (Table 2; Supplementary Table 3). Therefore, while apremilast gene regulation was focused on the inflammatory and immune response, cytokine and chemokine pathways, and stress response genes, cilomilast and roflumilast exhibited a broader pattern of gene regulation that included ribosomal genes, protein translation and disassembly, and the viral response genes. Confirmatory studies using quantitative real-time polymerase chain reaction analysis in LPS-stimulated monocytes found that apremilast (1 μM) significantly inhibited expression of

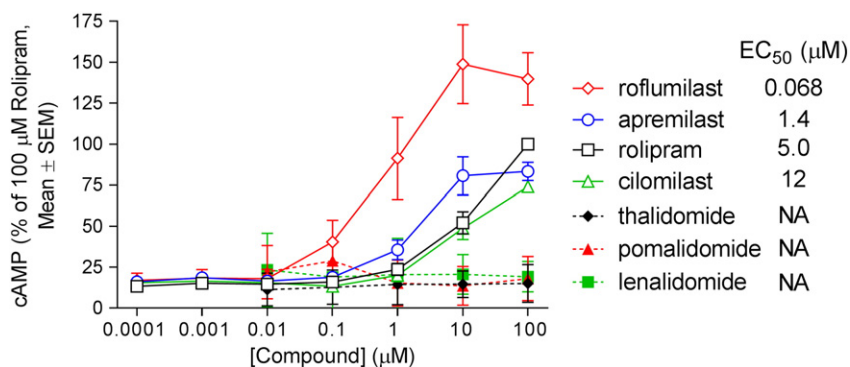


Fig. 3. Increase in intracellular cAMP levels by PDE4 inhibitors. Human PBMCs were pre-treated with compounds for 1 h, then stimulated with prostaglandin E2 for 1 h. Intracellular cAMP was measured by immunoassay and normalized to the level induced by prostaglandin E2 in the presence of 100 μM rolipram. Results shown are the average of three experiments performed in duplicate.

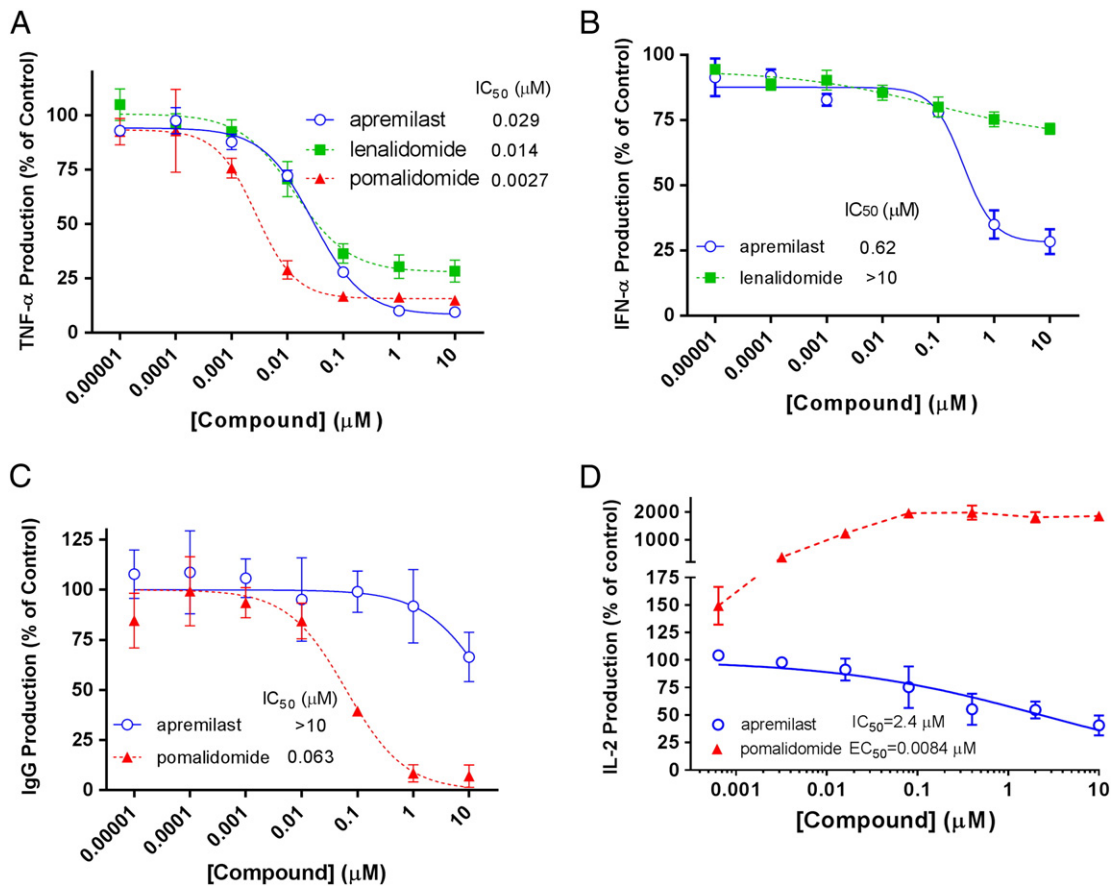


Fig. 4. Effect of apremilast and thalidomide analogs on innate and adaptive immune cells. A—TNF- α production from LPS-stimulated human PBMCs. B—CpG oligonucleotide-stimulated PBMCs. C—Effects of apremilast and pomalidomide on IgG secretion in normal PBMCs. Apremilast and pomalidomide + B-cell differentiating cocktail were added to normal PBMCs for 7 days. Cell culture supernatants were harvested and tested for human IgG by ELISA. The results were expressed as the percentage inhibition relative to control DMSO values and plotted versus concentration of test compound. D—Effects of apremilast and pomalidomide on T-cell production of IL-2. IC₅₀ values were calculated from the plots using non-linear regression, sigmoidal-dose response constraining the top to 100% and bottom to 0% allowing for a variable slope. The data points represent the mean of three experiments. Error bars represent the standard error of the mean.

interferon- γ by -8.64 -fold ($p < 0.01$) and significantly enhanced expression of suppressor of cytokine signaling 3 (SOCS-3) by 2.23 -fold ($p < 0.01$). In LPS-stimulated PBMCs, apremilast ($1 \mu\text{M}$) significantly inhibited expression of MCP-1 (CCL-2) by -5.04 -fold ($p < 0.01$), MCP-2 (CCL-8) by -21.3 -fold ($p < 0.001$), MIP-4 (CCL-18) by -46.3 -fold ($p < 0.01$), MIP-1 α R (CCR-1) by -6.38 -

fold ($p < 0.05$), interferon- γ by -15.2 -fold ($p < 0.05$), and TNF- α by -6.08 -fold ($p < 0.01$), but significantly up-regulated expression of amphiregulin by 2.07 -fold ($p < 0.05$), bone morphogenic protein 6 by -4.6 -fold ($p < 0.001$), and the chemokine epithelial-derived neutrophil-activating peptide 78 (CXCL-5) by 2.4 -fold ($p < 0.05$).

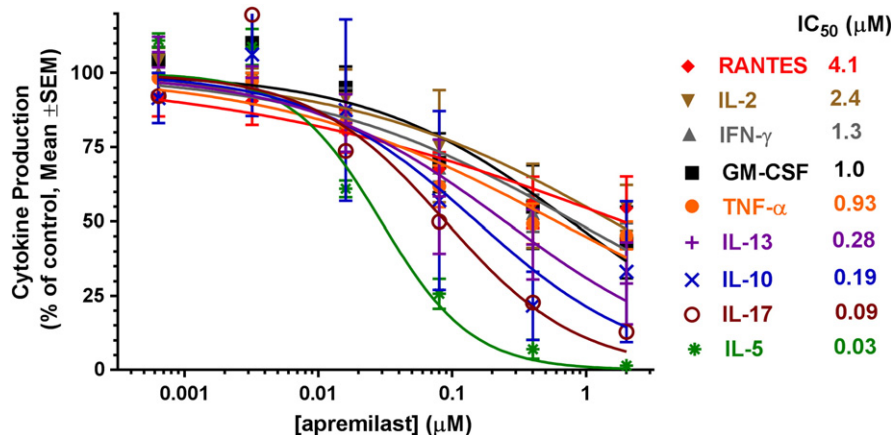


Fig. 5. Apremilast inhibition of Th1, Th2, and Th17 cytokines from primary human T cells stimulated via anti-CD3 antibody. Results were averaged using data from four separate T cell donors.

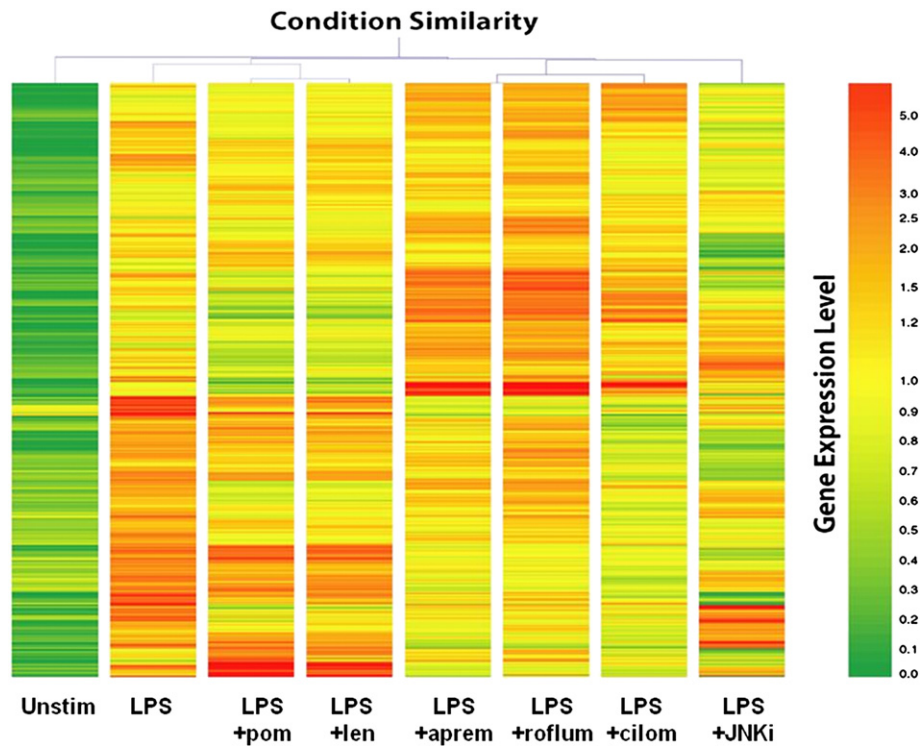


Fig. 6. Genome-wide gene expression analysis of LPS-stimulated primary human CD14+ monocytes treated with apremilast and the thalidomide analogs, lenalidomide and pomalidomide. Affymetrix U133A gene chips representing approximately 13,000 unique human genes were used. RNA was pooled from four separate donors, and replicate gene chips were run for each condition.

3.4. Intracellular signaling effects

The effects of apremilast were studied on Jurkat T cells and THP-1 monocytes in order to define the signaling pathways affected by PDE4 inhibition and cAMP elevation in immune inflammatory cells. Apremilast (1 and 10 μM), with and without forskolin 10 μM, significantly induced CREB phosphorylation at Ser133 in Jurkat T cells and, by contrast, roflumilast had a modest increase that was not significant (Fig. 7A). In THP-1

monocytic cells, apremilast showed a trend of increased CREB phosphorylation, but the increase was not statistically significant, while the PDE4 inhibitor roflumilast at 0.01 and 0.1 μM significantly increased CREB phosphorylation in THP-1 cells (Fig. 7B). Neither apremilast nor roflumilast had a significant effect on NF-κB nuclear localization in TNF-α-stimulated Jurkat T cells (Fig. 7C) or LPS-stimulated THP-1 monocytes (Fig. 7D).

Upon phosphorylation of CREB/ATF-1, these transcription factors bind to the cognate DNA sequence known as the cAMP responsive

Table 1

Top-scoring gene transcript biogroups regulated concordantly by PDE4 inhibitors in LPS-stimulated monocytes.

Compound	Common genes	Direction	p-Value	Score
<i>Immune response (GO)</i>				
Apremilast	45	↓	5.20E-16	118.14
Cilomilast	97	↓	5.60E-23	51.25
Roflumilast	36	↓	1.70E-14	31.70
<i>Inflammatory response (GO)</i>				
Apremilast	27	↓	7.80E-15	82.73
Cilomilast	34	↓	9.80E-12	32.49
Roflumilast	26	↓	1.60E-11	25.35
<i>Cytokine activity (GO)</i>				
Apremilast	20	↓	7.00E-14	67.70
Cilomilast	17	↓	3.90E-06	30.30
Roflumilast	15	↓	1.50E-11	12.46
<i>Chemokine signaling (Broad MSigDB – canonical pathways)</i>				
Apremilast	13	↓	2.80E-11	64.62
Cilomilast	22	↓	6.20E-10	24.31
Roflumilast	14	↓	5.00E-09	21.20
<i>Response to stress (GO)</i>				
Apremilast	72	↓	5.60E-09	64.52
Cilomilast	196	↓	1.70E-20	19.00
Roflumilast	71	↓	1.60E-07	45.52

LPS, lipopolysaccharide; MSigDB, Molecular Signatures Database.

Table 2

Top-scoring gene transcript biogroups regulated discordantly by apremilast versus other PDE4 inhibitors in LPS-stimulated monocytes.

Compound	Common genes	Direction	p-Value	Score
<i>Ribosome, cytoplasmic (Broad MSigDB – canonical pathways)</i>				
Apremilast	0		ns	96.05
Cilomilast	30	↑	1.30E-28	0.00
Roflumilast	22	↑	1.50E-14	64.21
<i>Peptide chain elongation (Broad MSigDB – canonical pathways)</i>				
Apremilast	0		ns	92.19
Cilomilast	30	↑	1.30E-27	0.00
Roflumilast	22	↑	7.30E-14	61.94
<i>Ribosome (Broad MSigDB – canonical pathways)</i>				
Apremilast	0		ns	90.71
Cilomilast	29	↑	1.00E-26	0.00
Roflumilast	22	↑	3.90E-14	59.84
<i>Protein complex disassembly (GO)</i>				
Apremilast	0		ns	86.74
Cilomilast	30	↑	3.10E-25	0.00
Roflumilast	24	↑	6.90E-14	56.43
<i>Viral infectious cycle (GO)</i>				
Apremilast	1	↓	ns	85.49
Cilomilast	30	↑	1.40E-23	1.69
Roflumilast	25	↑	2.80E-14	52.60

LPS, lipopolysaccharide; MSigDB, Molecular Signatures Database.

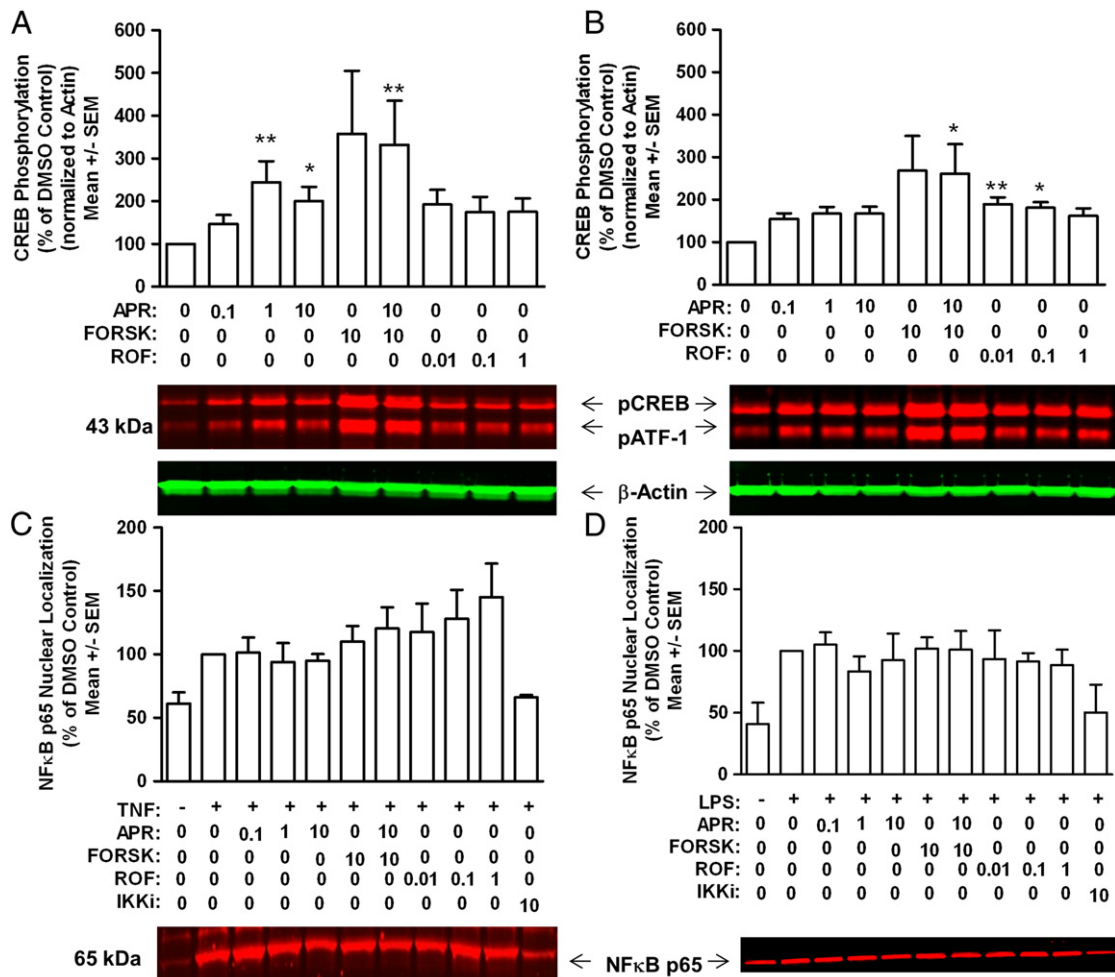


Fig. 7. Effect of Apremilast and Roflumilast on CREB phosphorylation and NF- κ B nuclear localization. A, B—Western blot analysis of CREB protein Ser133 phosphorylation in Jurkat T cells (A) and THP-1 monocytic cells (B). A representative Western blot is presented with each graph. All treatment groups were compared with DMSO by one-way ANOVA followed by Dunn's Multiple Comparison Post-Test ($n = 5$). No statistically significant difference was observed between Apremilast and Roflumilast. * $p < 0.05$ versus DMSO. ** $p < 0.01$ versus DMSO. 30-minute stimulation with drug. C, D—Western blot analysis of NF- κ B nuclear localization in Jurkat T cells stimulated with TNF- α over 1 h (C) and THP-1 monocytic cells stimulated with LPS over 1 h (D). A representative Western blot is presented along with each graph. Treatment groups were compared with TNF- α or LPS by one-way ANOVA followed by Dunnett's multiple comparison post-test ($n = 3$). No statistically significant difference was observed between Apremilast and Roflumilast or any other group.

element (CRE) and drive expression of CRE-dependent genes. Apremilast concentrations of 0.1, 1, and 10 μ M significantly enhanced CRE-driven transcriptional activity in Jurkat T cells (Fig. 8A) and THP-1 monocytes (Fig. 8B) at 6 h. At the same time, Apremilast significantly inhibited NF- κ B-driven transcriptional activity at 0.1, 1, and 10 μ M in both Jurkat (Fig. 8C) and THP-1 (Fig. 8D) cell lines.

3.5. Adaptive immune responses: antigen-specific transgenic T- and B-cell clonal expansion mouse model

To study the effect of Apremilast on the adaptive immune responses (i.e., antigen-specific clonal expansion and activation of T cells and B cells), the OVA-specific KJ1.26 + T-cell and HEL-specific IgMa + B-cell transfer mouse model was used. In this model, these transgenic T and B cells were transferred intravenously into a recipient mouse strain, and the conjugated peptide antigen OVA-HEL was injected subcutaneously, with or without treatment with Apremilast (5 mg/kg/day). This dose was similar to the dose used to demonstrate an anti-psoriatic effect in a xenograft mouse model [15], and much greater than the doses required to inhibit LPS-induced blood TNF- α levels in the rat (half-maximal effective dose [ED₅₀] 0.03 mg/kg), or to inhibit LPS-induced lung neutrophilia in the rat (ED₅₀ 0.3 mg/kg) [18].

Clonal expansion of KJ1.26 + T cells in the OVA-HEL immunized mice treated with vehicle control was first observed at Day 3 and continued through Day 5 to peak at 5% of lymphocytes on Day 7 (Fig. 9A). On each day after Day 2, the percentage of KJ1.26 + T cells was significantly higher in the OVA-HEL immunized group than in the unimmunized group ($p < 0.05$). Treatment with Apremilast did not affect this clonal expansion of the KJ1.26 + T cells at any time point (Fig. 9A).

The percentage of IgMa + B cells increased steadily during the experiment in OVA-HEL immunized mice treated with either Apremilast or vehicle (Fig. 9B). These cells constituted approximately 1.5% of the lymphocytes at the beginning of the study and finished at approximately 2%. On Days 5, 7, and 10, the percentage of IgMa + B cells in immunized mice was significantly higher than in unimmunized mice ($p < 0.05$). Apremilast had no effect on the number of IgMa + B cells at any of these time points (Fig. 9B).

Expression of the T-cell activation marker CD69 was detected upon 80% of KJ1.26 + T cells in OVA-HEL immunized mice treated on Day 2, but on only 25% of unimmunized mice ($p < 0.05$) (Fig. 9C). This CD69 expression was not affected by Apremilast in either the immunized or unimmunized animals. Approximately 45% of KJ1.26 + T cells in OVA-HEL immunized mice expressed the T-cell activation marker CD25 on Day 2, compared with only 3% of KJ1.26 + T cells from unimmunized

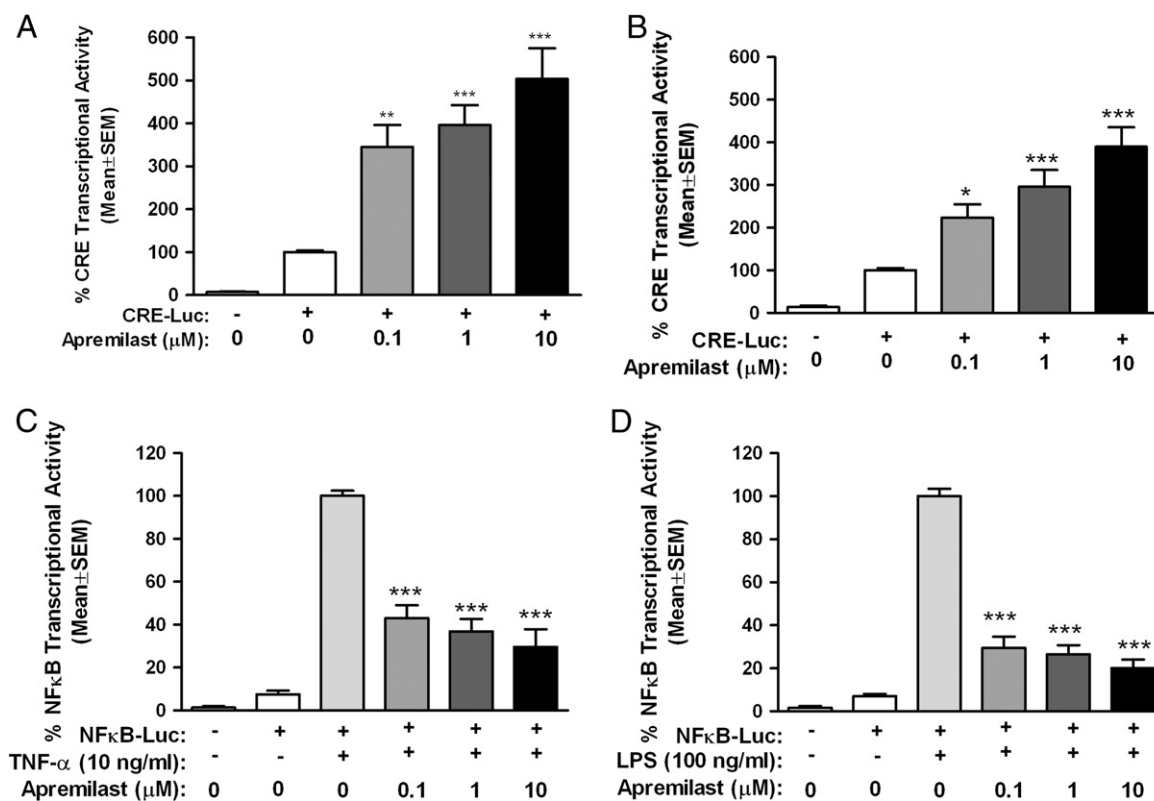


Fig. 8. A, B—Effect of apremilast on CRE-driven transcription in Jurkat T cells (A) and THP-1 monocytic cells (B) at 6 h. All treatment groups were compared with DMSO by one-way ANOVA followed by Dunnett's Multiple Comparison Post-Test ($n = 4$); * $p < 0.05$; ** $p < 0.01$; *** $p < 0.001$. C, D—Effect of apremilast on NF- κ B-driven transcriptional activity in Jurkat T cells (C) and THP-1 monocytic cells (D) at 6 h. All treatment groups were compared with TNF- α (C) or LPS (D) by one-way ANOVA followed by Dunnett's multiple comparison post-test ($n = 4$); *** $p < 0.001$ versus TNF- α or LPS.

mice ($p < 0.05$) (Fig. 9C). Apremilast had no significant effect on CD25 expression in either immunized or unimmunized mice. The T-cell activation marker CD62L, which typically decreases on activated cells, was reduced by immunization on Day 3 from 79% to 63%, although this decrease was not significant. In the immunized apremilast-treated group, CD62L expression was maintained at 79%, which was significantly higher than in the immunized vehicle control group. Therefore, a decrease in CD62L did not occur in the apremilast-treated immunized animals (Fig. 9C). Following restimulation of lymphocytes with OVA on Day 10, apremilast did not affect T-cell proliferation or interferon- γ production (data not shown).

For the B-cell activation marker CD80, no significant differences in the percentage of CD80^{high} Tg IgMa + B cells were noted on Day 3 and Day 5 between any of the treatment groups. On Day 7, the peak of CD80 expression, the unimmunized groups had significantly fewer CD80^{high} Tg IgMa + B cells than the immunized group treated with apremilast, but not the immunized control group. No significant difference in CD80 expression in the immunized mice was noted between apremilast and vehicle treatment (Fig. 9D). For CD86, on Day 3, significant differences were only encountered in the percentage of CD86^{high} Tg IgMa + B cells between unimmunized mice treated with either vehicle or apremilast and immunized mice treated with apremilast ($p < 0.05$). The immunized control was not significantly greater than the unimmunized control. On Day 5, the peak of CD86 expression, CD86^{high} Tg IgMa + B cells were observed to be higher in immunized groups compared with unimmunized groups ($p < 0.05$), but no significant differences were observed in immunized mice when comparing apremilast and vehicle treatment (Fig. 9D). By Day 7, statistically significant differences were only observed when comparing unimmunized vehicle-treated mice and immunized mice treated with either vehicle or apremilast ($p < 0.05$). For CD40, on Day 3 significant differences in

the percentage CD40^{high} IgMa + B cell populations were observed between unimmunized mice treated with vehicle and immunized mice treated with either vehicle or apremilast ($p < 0.05$). No significant differences were observed between unimmunized mice treated with apremilast and immunized mice treated with vehicle or apremilast, nor were there significant differences between immunized control-treated mice and their counterparts treated with apremilast. On Day 5, there were no significant differences between any of the treatment groups. On Day 7, the peak of CD40 expression, significant differences were encountered for unimmunized mice treated with vehicle and immunized mice treated with vehicle, but apremilast had no effect on CD40 expression (Fig. 9D). Overall, apremilast had no significant effect on CD80, CD86, or CD40 expression on IgMa + B cells on any day in the immunized mice compared with the immunized vehicle-treated mice. Production of OVA-specific IgG1, OVA-specific IgG2a, or HEL-specific IgMa was not affected by apremilast (data not shown).

3.6. Innate immune response and therapeutic index calculation: ferret lung neutrophilia versus gastrointestinal side effects

The conscious ferret model has been used to investigate anti-inflammatory, emetic, and behavioral effects of PDE4 inhibitors when administered by the oral route. Following apremilast dosing, significant ($p < 0.05$) inhibition of the lung neutrophilia was observed at 1, 10, and 30 mg/kg (62%, 70%, and 77%, respectively; Fig. 10A). Following compound dosing, the ferrets were observed for at least 2 h, and emetic episodes (retching and vomiting) and behavioral changes were recorded. Apremilast at doses < 10 mg/kg caused no emetic episodes (retching and vomiting). Some behavioral changes (flattened posture, lip licking, and backward walking) were observed and classified as mild. At 10 mg/kg in two of six ferrets, some retching but no frank emesis was

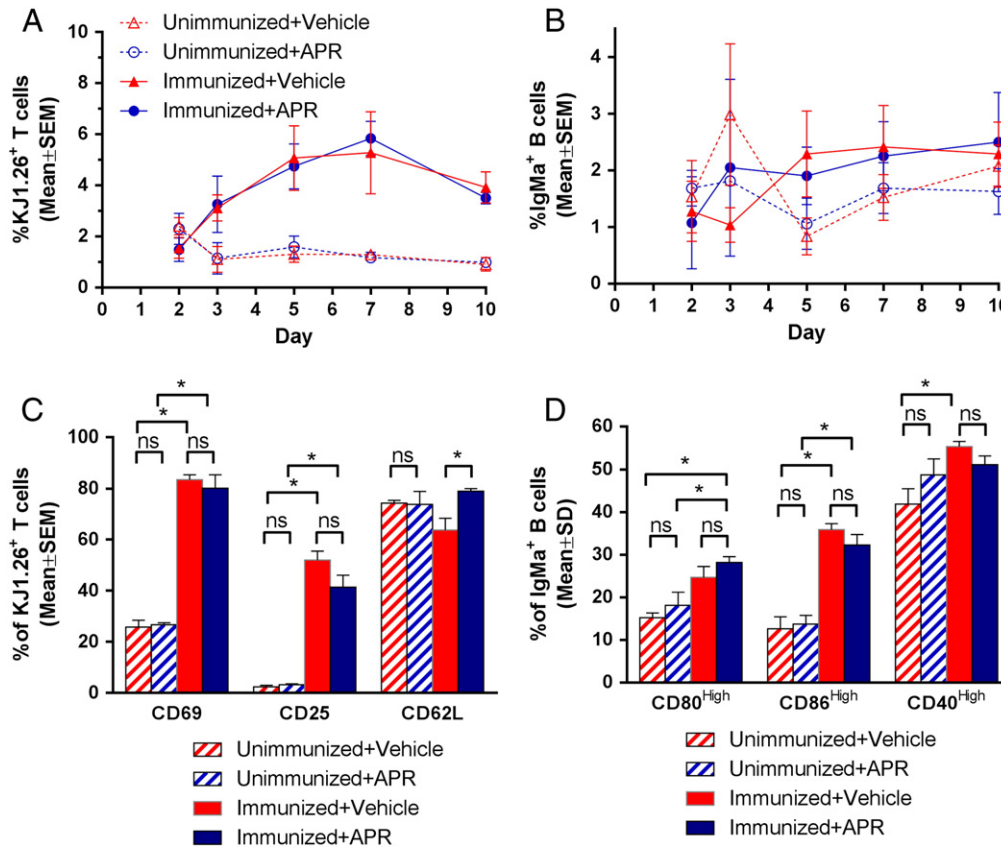


Fig. 9. A—T-cell expansion, as shown by percentage of KJ1.26⁺ cells in lymph nodes. B—B-cell expansion, as shown by percentage of IgMa⁺ cells in lymph nodes. C—T-cell activation markers on KJ1.26⁺ cells. **p* < 0.05 between the groups. D—Expression of B-cell activation markers on IgMa⁺ cells. **p* < 0.05 between the groups. Data points and bars represent the mean and standard error of the mean from five animals per time point.

observed along with salivation and behavioral changes (scored as mild or moderate), yielding an average of 0.5 episodes per animal. At the highest dose tested (30 mg/kg), moderate to marked emesis was observed in three of four animals along with pronounced behavioral changes. By comparison, cilomilast significantly inhibited lung neutrophils at 10 mg/kg by 51% (*p* < 0.05) (Fig. 10B). Regarding the number of emetic episodes, cilomilast induced retching and vomiting at doses of 3 to 10 mg/kg. From these experiments, a therapeutic index was determined by dividing the threshold dose for inducing emetic episodes by the ED₅₀ value for inhibiting the pulmonary neutrophilia. The therapeutic index values are summarized in Table 3. Of the compounds

evaluated, apremilast had the higher therapeutic index (12), causing no emetic episodes at an anti-inflammatory dose of 1 mg/kg. Cilomilast, by comparison, had a therapeutic index < 1 (0.38), indicating a 30-fold improvement in therapeutic index for apremilast compared with cilomilast.

4. Discussion

Apremilast is a PDE4 inhibitor that helps regulate the immune response that causes inflammation associated with PsA and psoriasis. In the current report, enzyme assays confirm that apremilast is a specific

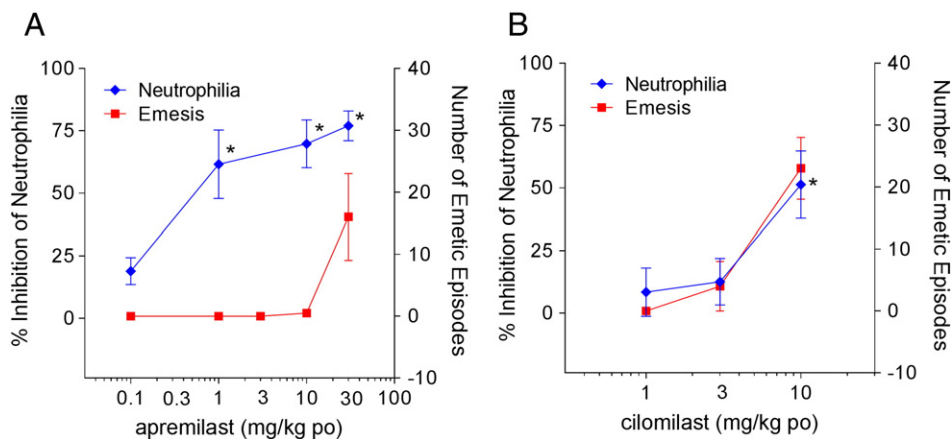


Fig. 10. Ferret lung neutrophilia and emesis model results with apremilast and cilomilast. **p* < 0.05 for inhibition of lung neutrophilia. Data are the mean ± standard error from four to eight animals.

Table 3

Therapeutic index for apremilast and cilomilast based on inhibition of neutrophilia and emetic dose in the ferret.

Compound	Inhibition of LPS-induced neutrophilia (ED ₅₀ mg/kg)	Threshold emetic dose (mg/kg)	Therapeutic index
Apremilast	0.8	10	12
Cilomilast	8	3	0.38

ED₅₀, dose producing a response that is 50% of the maximum obtainable.

PDE4 inhibitor and non-selective for PDE4 subtypes. With the exception of PDE4, apremilast did not significantly inhibit any of the kinases tested and had no significant activity against any of the cell surface receptors or enzymes tested. Therefore, the only known molecular targets of apremilast are the PDE4 family of enzymes.

Apremilast is able to potently bind and inhibit PDE4 because it contains the dialkoxyphenyl pharmacophore [18]. The dialkoxyphenyl group is found in several other PDE4 inhibitors, which have been clinically tested or are approved [46–48]. By contrast, thalidomide and its functional analogs, the IMiDs® compounds, lenalidomide and pomalidomide, bind to cereblon, an E3 ubiquitin ligase substrate co-receptor protein encoded by the gene *CRBN* [39,44]. Cereblon has been shown to mediate the antiproliferative effect of lenalidomide and pomalidomide against multiple myeloma cells, as well as their T-cell co-stimulatory effects [44]. Also, in embryonic development models using zebrafish and chick embryos, cereblon binding was found to mediate the teratogenic effects of thalidomide [39]. The key pharmacophore for thalidomide, lenalidomide, and pomalidomide is the glutarimide ring; this ring mediates the binding of thalidomide, lenalidomide, and pomalidomide to cereblon [39,44]. Because apremilast does not contain a glutarimide ring, the inability of apremilast to bind to cereblon (Fig. 2) was an expected result.

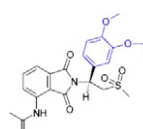
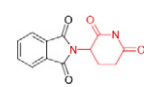
Apremilast also contains another chemical group, the isoindolinone group (also known as the phthalimide group) [18]. This phthalimide group does not control binding to cereblon [39,44]. Before the discovery of cereblon, the molecular mechanism of action of thalidomide was not known, and it was not known which part of the molecule was responsible for its pharmacological function. Thus, in older publications, compounds containing the phthalimide group were sometimes referred to as “thalidomide analogs” [49]. Since it is now understood that thalidomide binding to cereblon is mediated through the glutarimide ring [39,44], apremilast is no longer considered to be a functional analog of thalidomide.

In addition to having a different structure and function than thalidomide, lenalidomide, and pomalidomide, apremilast also has very different pharmacological effects in cells. For example, while thalidomide and its analogs, lenalidomide and pomalidomide, enhance the activity of T cells [45] and NK cells [50], apremilast has the opposite effect, and it actually inhibits the cytokine production by T cells (Figs. 4 and 5) and NK cells [15]. A summary of the structural and pharmacological differences between apremilast and the thalidomide analogs is provided in Table 4.

The immunopathophysiology of inflammatory diseases such as psoriasis and arthritis is complex, involving cells of both the innate immune system, such as monocytes and DCs, and the adaptive immune provided by T cells and B cells [1,2]. Plasmacytoid DCs are key sentinels that, when activated through TLR ligands, produce the type 1 interferon- α , resulting in myeloid DC and T-cell activation [1–3,51]. Apremilast 10 μ M efficiently inhibited interferon- α by TLR9 ligand-stimulated PBMCs by approximately 75%. These findings are consistent with previous reports that apremilast suppresses expression of MX1 mRNA, a marker of the type 1 interferon response in skin lesions from patients enrolled in an open-label phase II apremilast study in recalcitrant psoriasis [24]. Another notable observation in the current study is the inhibition of IL-17 production by purified T cells (IC₅₀ 90 nM) (Fig. 5). This, too, was confirmed in the recalcitrant psoriasis study, wherein apremilast treatment resulted in a median 72.5% reduction of IL-17A

Table 4

Comparison of structural and pharmacological differences between apremilast and thalidomide and the IMiDs® compounds, lenalidomide and pomalidomide.

	Apremilast	Thalidomide, lenalidomide, and pomalidomide
		
Key chemical group	Dialkoxyphenyl ring (blue)	Amino-glutarimide ring (red)
PDE4 binding	Yes	No
Increase in cyclic AMP	Yes	No
Inhibit T and NK cells	Yes	No
Cereblon binding	No	Yes
Inhibit B cells	No	Yes
Co-stimulate T and NK cells	No	Yes

^aAmino-glutarimide ring (red) of the thalidomide structure is also part of the structure of lenalidomide and pomalidomide.

mRNA in skin lesions after 4 weeks [24]. This direct inhibition of IL-17 production is important, given the crucial role that Th17 cells play in the pathophysiology of psoriasis [52].

Differentiation of B cells to antibody-producing plasma cells is another important component of the autoimmune and inflammatory responses in diseases such as rheumatoid arthritis [53]. Our study demonstrated that the effects of apremilast on B-cell differentiation are weak. Apremilast did not significantly inhibit IgG (Fig. 4C) or IgM production (data not shown) in normal B-cell differentiation cultures. This finding suggests that the effects of apremilast on adaptive immunity may be minor, especially compared with the reduction of innate immune responses seen against monocytes, neutrophils, and NK cells [15]. Indeed, this observation was confirmed *in vivo* using the antigen-specific mouse B-cell transfer model, wherein no effects of apremilast on B-cell activation were observed (Fig. 9).

In the gene chip analysis, clear differences in gene expression were noted between apremilast and the thalidomide analogs, lenalidomide and pomalidomide. Gene expression studies in LPS-stimulated human PBMCs and monocytes identified several targets of gene regulation by apremilast, including the inhibition of many chemokines, chemokine receptors, and Th1 cytokine genes, as well as enhancement of the genes encoding the anti-inflammatory factor SOCS-3. SOCS-3 is an inhibitor of the cytokine receptor/JAK-STAT pathway and has previously been observed to be induced by cAMP elevation via the activation of Epac1 (exchange protein directly activated by cAMP 1) [54]. Thus, apremilast may be able to suppress cytokine signaling through the IL-6 and other class I cytokine receptors, through activation of Epac1, expression of SOCS-3, and inhibition of JAK-STAT signaling.

Through increases in intracellular cAMP, PDE4 inhibitors lead to phosphorylation and activation of PKA [15]. This results in up-regulation of CREB and down-regulation of NF- κ B-dependent genes [14,15]. The current data from Western blot analyses show that apremilast significantly induces CREB phosphorylation, which is indicative of PKA activation. Apremilast significantly enhanced CRE-driven gene transcription in Jurkat T cells and THP-1 monocytic cells, which can subsequently induce transcription of genes such as IL-10 and IL-6 [15]. These findings are consistent with CREB phosphorylation observed by Western blot and confirm that apremilast activates the PKA pathway in these cells. In addition, apremilast inhibits NF- κ B transcriptional activity, which drives expression of genes such as TNF- α [15]. The

inhibitory action of the cAMP/PKA pathway on the transcriptional activity of NF- κ B is mediated either by a competition for CREB-binding protein [55], or via a direct or indirect modification of the C-terminal transactivation domain of NF- κ B p65 [56]. Our studies show that apremilast does indeed induce phosphorylation of the PKA substrates CREB and ATF-1, induce CRE-dependent transcriptional activity, and inhibit NF- κ B transcriptional activity without affecting nuclear translocation of NF- κ B. These data are consistent with either the CREB-binding protein-dependent or CREB-binding protein-independent model of NF- κ B inhibition. Interestingly, our results suggest that there may be differences between apremilast and roflumilast with respect to CREB phosphorylation in Jurkat T cells and THP-1 monocytic cells; these potential distinctions are being explored further in additional studies.

5. Conclusions

The current analyses confirm that apremilast is a selective inhibitor of PDE4 that works intracellularly to regulate inflammatory mediators. Apremilast activates the PKA-CREB/ATF-1 pathway, resulting in enhancement of CRE-driven gene transcription and inhibition of NF- κ B-driven gene transcription. Unlike thalidomide or its analogs, lenalidomide and pomalidomide, apremilast does not bind to human cereblon and shows clear differences from these drugs in cellular pharmacology and gene expression studies. Unlike pomalidomide, apremilast showed minimal effects on B-cell differentiation and immunoglobulin production, supporting previous findings that the effects of apremilast on innate immunity are greater than those on adaptive immunity. Despite having an inhibitory effect on Th1, Th2, and Th17 cytokine production, there was no effect of apremilast on T-cell or B-cell clonal expansion (Fig. 9), or on antibody responses in vivo (data not shown). These findings may explain the low risk of serious infection and overall safety profile reported in clinical studies to date [20,25,26,57]. Long-term use of currently available non-biologic and biologic systemic therapies is often compromised by adverse events, safety and tolerability issues, loss of effect over time, and administration by injection [3,58]. Treatment options are needed that are efficacious, safe, well tolerated, and easy to use. In the ferret pharmacology/tolerability model measuring an innate immune response and the known PDE4 inhibitor-mediated gastrointestinal side effects (nausea and vomiting), apremilast demonstrated a significant anti-inflammatory effect with a >10-fold margin compared with the onset of side effects, representing a 30-fold improvement over cilomilast, another PDE4 inhibitor that had been previously been in clinical development. These nonclinical pharmacology and tolerability results provide support regarding why apremilast may represent an important new oral treatment option for patients with inflammatory conditions.

In phase III studies, apremilast was effective and well tolerated in the treatment of psoriasis and PsA [29–33]. In the ESTEEM 1 study, apremilast significantly improved Psoriasis Area and Severity Index scores in patients with moderate to severe plaque psoriasis; after 16 weeks, a significantly greater proportion of patients receiving apremilast 30 mg BID (33%) achieved a 75% reduction from baseline Psoriasis Area and Severity Index score compared with those receiving placebo (5%; $p < 0.0001$ versus placebo) [29]. In the PALACE 1 study (the first study from the PALACE clinical trial program), patients with active PsA achieved 20% improvement in modified American College of Rheumatology response criteria at 16 weeks at a significantly greater rate with apremilast 20 mg BID (31%; $p < 0.02$) and apremilast 30 mg BID (40%; $p = 0.0001$) compared with placebo (19%) [30]. In a pooled safety analysis of the PALACE 1, PALACE 2, and PALACE 3 studies, the most common adverse events were diarrhea, nausea, headache, upper respiratory tract infection, and nasopharyngitis [59]. Most adverse events were mild to moderate in severity, and discontinuations due to adverse events were low [59]. In addition, no relevant safety signals for opportunistic infection, cancer, demyelination, or lupus-like syndromes have been attributed to apremilast to date. There also have

been no indications of significant laboratory or electrocardiographic abnormalities or clinically significant effects on liver function, white blood cells, blood pressure, or hemoglobin. Additional results from the PALACE 2, PALACE 3, and PALACE 4 studies demonstrate the clinical efficacy of apremilast in patients with active PsA, with no new safety signals observed and improved tolerability over phase II studies [27, 31–33,60].

Supplementary data to this article can be found online at <http://dx.doi.org/10.1016/j.cellsig.2014.05.014>.

Conflicts of interest

P.H. Schafer, A. Parton, L. Capone, D. Cedzik, H. Brady, H.-W. Man, and R. Chopra are employees of Celgene Corporation.

Acknowledgments

This research was supported by Celgene Corporation. The authors received editorial support in the preparation of this manuscript from Vrinda Mahajan, PharmD, of Peloton Advantage, LLC, and Jennifer Schwinn, RPh, funded by Celgene Corporation.

References

- [1] M.A. Lowes, A.M. Bowcock, J.G. Krueger, *Nature* 445 (2007) 866–873.
- [2] F.O. Nestle, D.H. Kaplan, J. Barker, *N. Engl. J. Med.* 361 (2009) 496–509.
- [3] P. Schafer, *Biochem. Pharmacol.* 83 (2012) 1583–1590.
- [4] M. Conti, J. Beavo, *Annu. Rev. Biochem.* 76 (2007) 481–511.
- [5] C.H. Serezani, M.N. Ballinger, D.M. Aronoff, M. Peters-Golden, *Am. J. Respir. Cell Mol. Biol.* 39 (2008) 127–132.
- [6] A.C. Zambon, L. Zhang, S. Minovitsky, J.R. Kanter, S. Prabhakar, N. Salomonis, K. Vranizan, I. Dubchak, B.R. Conklin, P.A. Insel, *Proc. Natl. Acad. Sci. U. S. A.* 102 (2005) 8561–8566.
- [7] V. Ollivier, G.C. Parry, R.R. Cobb, D. de Prost, N. Mackman, *J. Biol. Chem.* 271 (1996) 20828–20835.
- [8] J.L. Jimenez, C. Punzon, J. Navarro, M.A. Munoz-Fernandez, M. Fresno, *J. Pharmacol. Exp. Ther.* 299 (2001) 753–759.
- [9] S.H. Francis, M.A. Blount, J.D. Corbin, *Physiol. Rev.* 91 (2011) 651–690.
- [10] P. Salari, M. Abdollahi, *Expert. Opin. Investig. Drugs* 21 (2012) 261–264.
- [11] P.H. Schafer, Presented at: 8th International Congress on Autoimmunity; May 9–13; Granada, Spain, 2012.
- [12] M.D. Houslay, *Trends Biochem. Sci.* 35 (2010) 91–100.
- [13] M.D. Houslay, G.S. Baillie, D.H. Maurice, *Circ. Res.* 100 (2007) 950–966.
- [14] M.D. Houslay, P. Schafer, K.Y. Zhang, *Drug Discov. Today* 10 (2005) 1503–1519.
- [15] P.H. Schafer, A. Parton, A.K. Gandhi, L. Capone, M. Adams, L. Wu, J.B. Bartlett, M.A. Loveland, A. Gilhar, Y.-F. Cheung, G.S. Baillie, M.D. Houslay, H.-W. Man, G.W. Muller, D.J. Stirling, *Br. J. Pharmacol.* 159 (2010) 842–855.
- [16] Otezla (apremilast) [package insert], Celgene Corporation, Summit, NJ, March 2014.
- [17] Daliresp (roflumilast) [package insert], Forest Pharmaceuticals, Inc., St. Louis, MO, August 2013.
- [18] H.-W. Man, P. Schafer, L.M. Wong, R.T. Patterson, L.G. Corral, H. Raymon, K. Blease, J. Leisten, M.A. Shirley, Y. Tang, D.M. Babusis, R. Chen, D. Stirling, G.W. Muller, *J. Med. Chem.* 52 (2009) 1522–1524.
- [19] L. Capone, A. Rogovitz, A.K. Gandhi, P.H. Schafer, *Arthritis Rheum.* 63 (10 Suppl.) (2011) 1844.
- [20] A.B. Gottlieb, B. Strober, J.G. Krueger, P. Rohane, J.B. Zeldis, C.C. Hu, C. Kipnis, *Curr. Med. Res. Opin.* 24 (2008) 1529–1538.
- [21] F.E. McCann, A.C. Palfreeman, M. Andrews, D.P. Perocheau, J.J. Inglis, P. Schafer, M. Feldman, R.O. Williams, F.M. Brennan, *Arthritis Res. Ther.* 12 (2010) R107.
- [22] L. Wu, M. Adams, S. Parton, P.H. Schafer, *Arthritis Rheum.* 64 (2012) S20.
- [23] M. Adams, P.H. Schafer, *Arthritis Rheum.* 64 (2012) S17.
- [24] A.B. Gottlieb, R.T. Matheson, A. Menter, C.L. Leonardi, R.M. Day, C.C. Hu, P.H. Schafer, J.G. Krueger, *J. Drugs Dermatol.* 12 (2013) 888–897.
- [25] K. Papp, J. Cather, L. Rosoph, H. Sofen, R.G. Langley, R.T. Matheson, A. Hu, R.M. Day, *Lancet* 380 (2012) 738–746.
- [26] G. Schett, J. Wollenhaupt, K. Papp, R. Joos, K.L. DeVlam, J.F. Rodrigues, A. Vessey, C.C. Hu, R. Stevens, *Arthritis Rheum.* 64 (2012) 3156–3167.
- [27] Celgene Biopharmaceutical, Apremilast PALACE program demonstrates robust and consistent statistically significant clinical benefit across three pivotal phase III studies (PALACE-1, 2 & 3) in psoriatic arthritis [press release], Available at: <http://ir.celgene.com/phoenix.zhtml?c=111960&p=irol-newsArticle&ID=1732178&highlight=2013> (Accessed September 10, 2013).
- [28] G. Hatemi, M. Melikoglu, R. Tunc, C. Korkmaz, B.T. Ozturk, C. Mat, P.A. Merkel, K. Calamia, Z. Liu, L. Pineda, R.M. Stevens, H. Yazici, Y. Yazici, *Arthritis Rheum.* 65 (10 Suppl.) (2013) S322.
- [29] K. Reich, K. Papp, C. Leonardi, L. Kircik, S. Chimenti, C.C. Hu, R.M. Stevens, R.M. Day, C.E.M. Griffiths, Presented at: Annual Meeting of the American Academy of Dermatology; March 1–5, Miami, FL, 2013.

- [30] A. Kavanaugh, P.J. Mease, A. Adebajo, J. Wollenhaupt, C.C. Hu, K. Shah, R.M. Stevens, J.J. Gomez-Reino, Presented at: Annual Congress of the European League Against Rheumatism; June 12–15, Madrid, Spain, 2013.
- [31] M. Cutolo, G.E. Myerson, R.M. Fleischmann, F. Liote, F. Diaz-Gonzalez, F. Van den Bosch, H. Marzo-Ortega, E. Feist, K. Shah, C.C. Hu, R.M. Stevens, A. Poder, *Arthritis Rheum.* 65 (10 Suppl.) (2013) S346–S347.
- [32] C.J. Edwards, F.J. Blanco, J. Crowley, C.C. Hu, R.M. Stevens, C.A. Birbara, *Arthritis Rheum.* 65 (10 Suppl.) (2013) S132.
- [33] A.F. Wells, C.J. Edwards, A.O. Adebajo, A.J. Kivitz, P. Bird, K. Shah, C.C. Hu, R.M. Stevens, J.A. Aelion, Presented at: Annual Scientific Meeting of the American College of Rheumatology; October 26–30, San Diego, CA, 2013.
- [34] G. Nemoz, C. Sette, M. Conti, *Mol. Pharmacol.* 51 (1997) 242–249.
- [35] M. Sullivan, A.S. Olsen, M.D. Houslay, *Cell. Signal.* 11 (1999) 735–742.
- [36] M.M. McLaughlin, L.B. Cieslinski, M. Burman, T.J. Torphy, G.P. Livi, *J. Biol. Chem.* 268 (1993) 6470–6476.
- [37] G. Nemoz, R. Zhang, C. Sette, M. Conti, *FEBS Lett.* 384 (1996) 97–102.
- [38] M. Sullivan, G. Rena, F. Begg, L. Gordon, A.S. Olsen, M.D. Houslay, *Biochem. J.* 333 (Pt 3) (1998) 693–703.
- [39] T. Ito, H. Ando, T. Suzuki, T. Ogura, K. Hotta, Y. Imamura, Y. Yamaguchi, H. Handa, *Science* 327 (2010) 1345–1350.
- [40] C.L. Adams, C.M. Rush, K.M. Smith, P. Garside, *Methods Mol. Biol.* 239 (2004) 133–146.
- [41] R. Barber, G.S. Baillie, R. Bergmann, M.C. Shepherd, R. Sepper, M.D. Houslay, G.V. Heeke, *Am. J. Physiol. Lung Cell. Mol. Physiol.* 287 (2004) L332–L343.
- [42] E. Huston, T.M. Houslay, G.S. Baillie, M.D. Houslay, *Biochem. Soc. Trans.* 34 (2006) 504–509.
- [43] G. Molostvov, A. Morris, P. Rose, S. Basu, G. Muller, *Br. J. Haematol.* 124 (2004) 366–375.
- [44] A. Lopez-Girona, D. Mendy, T. Ito, K. Miller, A.K. Gandhi, J. Kang, S. Karasawa, G. Carmel, P. Jackson, M. Abbasian, A. Mahmoudi, B. Cathers, E. Rychak, S. Gaidarova, R. Chen, P.H. Schafer, H. Handa, T.O. Daniel, J.F. Evans, R. Chopra, *Leukemia* 26 (2012) 2326–2335.
- [45] L.G. Corral, P.A. Haslett, G.W. Muller, R. Chen, L.M. Wong, C.J. Ocampo, R.T. Patterson, D.I. Stirling, G. Kaplan, *J. Immunol.* 163 (1999) 380–386.
- [46] J.M. McKenna, G.W. Muller, in: J.A. Beavo, S.H. Francis, M.D. Houslay (Eds.), *Cyclic Nucleotide Phosphodiesterases in Health and Disease*, CRC Press/Taylor & Francis, Boca Raton, FL, 2007, pp. 667–699.
- [47] A. Kodimuthali, S.S. Jabaris, M. Pal, *J. Med. Chem.* 51 (2008) 5471–5489.
- [48] H. Tenor, A. Hatzelmann, R. Beume, G. Lahu, K. Zech, T.D. Bethke, *Handb. Exp. Pharmacol.* (2011) 85–119.
- [49] G.W. Muller, M.G. Shire, L.M. Wong, L.G. Corral, R.T. Patterson, Y. Chen, D.I. Stirling, *Bioorg. Med. Chem. Lett.* 8 (1998) 2669–2674.
- [50] L. Wu, M. Adams, T. Carter, R. Chen, G. Muller, D. Stirling, P. Schafer, J.B. Bartlett, *Clin. Cancer Res.* 14 (2008) 4650–4657.
- [51] L.C. Zaba, J. Fuentes-Duculan, N.J. Eungdamrong, L.M. Johnson-Huang, K.E. Nograles, T.R. White, K.C. Pierson, T. Lentini, M. Suarez-Farinas, M.A. Lowes, J.G. Krueger, *J. Allergy Clin. Immunol.* 125 (2010) 1261–1268.
- [52] J.G. Krueger, S. Fretzin, M. Suarez-Farinas, P.A. Haslett, K.M. Phipps, G.S. Cameron, J. McColm, A. Katcharian, I. Cueto, T. White, S. Banerjee, R.W. Hoffman, *J. Allergy Clin. Immunol.* 130 (2012) 145–154.
- [53] J.D. Bouaziz, K. Yanaba, T.F. Tedder, *Immunol. Rev.* 224 (2008) 201–214.
- [54] J.J. Williams, T.M. Palmer, *Biochem. Soc. Trans.* 40 (2012) 215–218.
- [55] G.C. Parry, N. Mackman, *J. Immunol.* 159 (1997) 5450–5456.
- [56] N. Takahashi, T. Tetsuka, H. Uranishi, T. Okamoto, *Eur. J. Biochem.* 269 (2002) 4559–4565.
- [57] P.H. Schafer, Presented at: 41st Annual Meeting of the European Society for Dermatological Research; September 7–12, Barcelona, Spain, 2011.
- [58] A. Menter, N.J. Korman, C.A. Elmets, S.R. Feldman, J.M. Gelfand, K.B. Gordon, A.B. Gottlieb, J.Y.M. Koo, M. Lebwohl, H.W. Lim, A.S. Van Voorhees, K.R. Beutner, R. Bhushan, *J. Am. Acad. Dermatol.* 61 (2009) 451–485.
- [59] P.J. Mease, A. Kavanaugh, D.D. Gladman, A.O. Adebajo, J.J. Gomez-Reino, J. Wollenhaupt, M. Cutolo, G. Schett, E. Lespessailles, K. Shah, C.C. Hu, R.M. Stevens, C.J. Edwards, C.A. Birbara, *Arthritis Rheum.* 65 (10 Suppl.) (2013) S131–S132.
- [60] Celgene International Sarl, Apremilast achieves statistical significance for the primary endpoint of the first phase III study (PALACE-1) in patients with psoriatic arthritis [press release], Available at: <http://ir.celgene.com/phoenix.zhtml?c=111960&p=iroil-newsArticle&iD=1714113&highlight=> (Accessed August 6, 2013).